Adaptive Sampling and Non Linear Reconstruction for Cardiac Magnetic Resonance Imaging

Giuseppe Placidi[1], Danilo Avola[1], Luigi Cinque[2], Guido Macchiarelli[1], Andrea Petracca[1], and Matteo Spezialetti[1]

[1] Department of Life, Health and Environmental Sciences, University of L'Aquila
Via Vetoio Coppito 2, 67100, L'Aquila, Italy
{giuseppe.placidi,danilo.avola,andrea.petracca,
matteo.spezzialetti}@univaq.it, guido.macchiarelli@cc.univaq.it
[2] Department of Computer Science, Sapienza University
Via Salaria 113, 00198, Rome, Italy
cinque@di.uniroma1.it

Abstract. We show how an adaptive acquisition sequence and a non linear reconstruction can be efficiently used to reconstruct undersampled cardiac MRI data. We demonstrate that, by using the adaptive method and L_0-homotopic minimization, we can reconstruct an image with a number of samples which is very close to the sparsity coefficient of the image without knowing a-priori the sparsity of the image. We highlight two important aspects: 1) how the shape and the cardinality of the starting dataset influence the acquisition/reconstruction process; 2) how well the termination criteria allows to fit the optimal number of coefficients. The method is tested on MRI cardiac images and it is also compared to the weighted Compressed Sensing. All the experiments and results are reported and discussed.

Keywords: adaptive sampling, compressed sensing, non linear reconstruction, MRI, cardiac imaging, image reconstruction, imaging.

1 Introduction

Magnetic Resonance Imaging (MRI) has become a major non-invasive imaging modality due to its ability to provide structural details of human body and additional functional information. Cardiac imaging, in particular, represents one of the challenging applications where MRI can be effectively used. Being cardiac imaging a dynamic application, particular triggering techniques have to be used to avoid motion artifacts. However, acquisition time is usually long if a complete set of k-space trajectories has to be collected [1]. In order to decrease acquisition time, a reduced number of trajectories could be accepted through undersampling.

Undersampling is the violation of the Nyquist's criterion where images are reconstructed by using a number of samples lower than what is theoretically required to obtain a fully sampled image. Some methods [2], [3], [4] presented

Y.J. Zhang and J.M.R.S. Tavares (Eds.): CompIMAGE 2014, LNCS 8641, pp. 24–35, 2014.

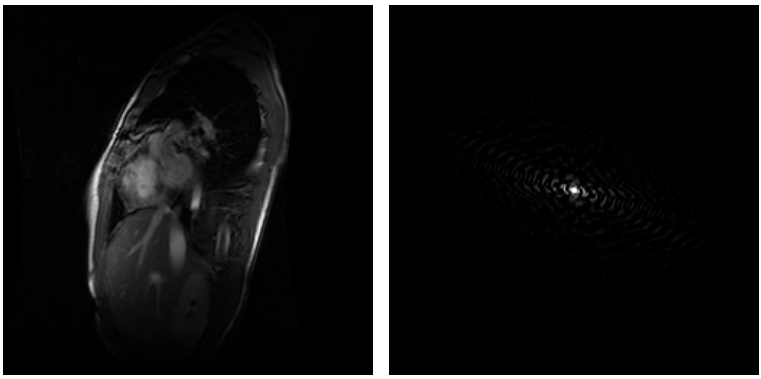

Fig. 1. Original cardiac image (a) and its Fourier coefficients (b) choosen as k-space samples

adaptive acquisition techniques for MRI from projections. One of these [4] defined the entropy function on the power spectrum of the collected projections to evaluate their information content, thus driving the acquisition where data variability is maximum. The choice of the projections was made during the acquisition process; this allowed the reduction of acquisition time, by reducing the scanned directions. A modified Fourier reconstruction algorithm, including an interpolation method [5], was used to reconstruct the image from the sparse set of projections. Other authors [6], [7], [8], [9], [10] presented the theory of Compressed Sensing (CS) and the details of its implementation for rapid MRI and demonstrated that if an image is sparse in some domain, then it can be recovered from randomly undersampled raw data, having supposed that a non linear reconstruction algorithm is used. A well-performant non linear reconstruction algorithm has been proposed in [11] and [12] and it is based on homotopic approximation of the L_0-norm. Non linear reconstruction can also be improved by increasing samples in the central region of the k-space where low frequency terms contain most of the energy of the image, as demonstrated in weighed CS [13], [14].

In the present paper we show how an adaptive acquisition sequence and non linear reconstruction [15], [16] can be efficiently used to reconstruct undersampled cardiac MRI data. Moreover, it is discussed how the adaptive method is effective in collecting the near optimal number of data to reconstruct the unknown image (at least two times lower than the number fixed by CS) and how the termination strategy is capable to stop the acquisition just to the correct number, adapted to the image shape. Numerical simulations are reported and compared with weighted CS to show its performances.

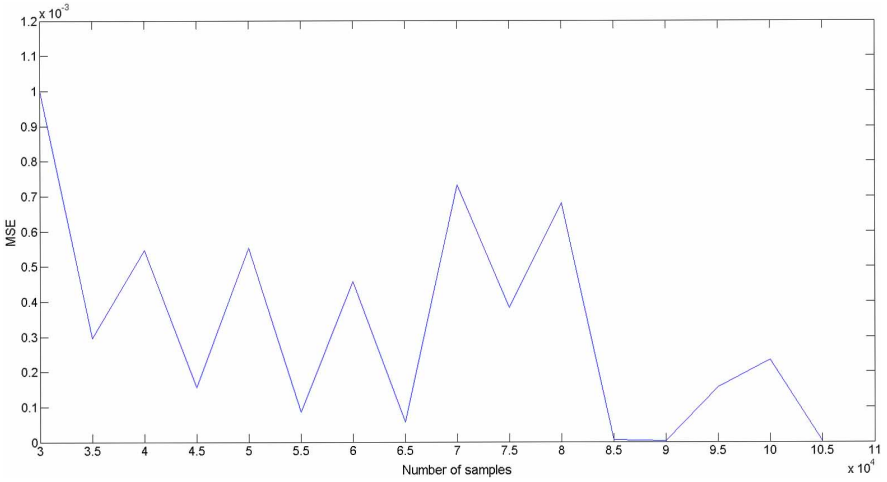

(a)

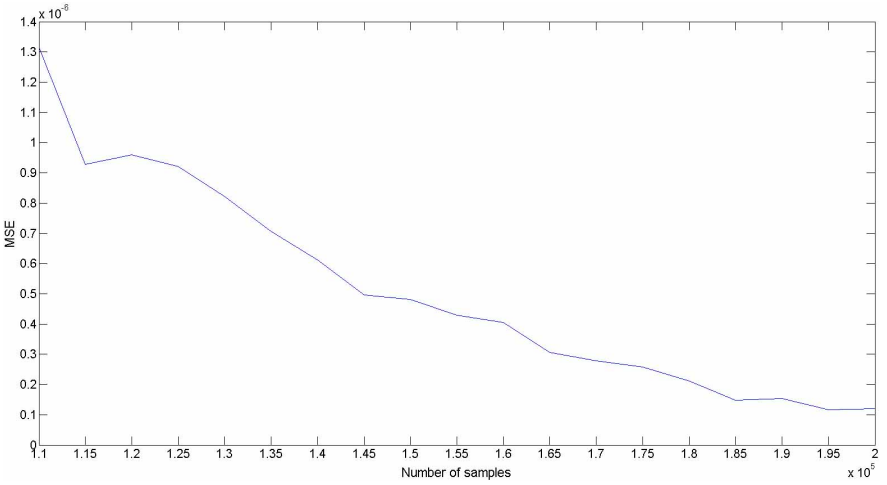

(b)

Fig. 2. MSE values calculated on the CS images reconstructed by using increasing datasets from 30000 to 200000 samples (by steps of 5000). The plot is divided in two to appreciate MSE amplitude variations.

2 The Acquisition/Reconstruction Method

The used adaptive acquisition method, described in [15], consists of two phases. Consider the k-space image support as a M × M matrix. In a first phase, the acquisition process collects a set of random Cartesian trajectories, having a Gaussian distribution in a central region of the k-space whose width is a portion p

(a) (b)

Fig. 3. CS reconstruction with 115000 samples (a) and difference between the theoretical image (Figure 1(a)) and CS reconstruction (b)

of the k-space, both along the rows and along the columns. Each trajectory is completely sampled but the number of total trajectories is lower than p. Lines are collected by randomizing the phase-encoding gradient and the columns are collected by reversing the phase-encoding gradient with the frequency-encoding gradient (also in this case, the randomization process involves phase-encoding). The square central region W, whose size is p $\times$ p, provides the foundation for the proposed adaptive sampling where an equispaced set of 20 radial projections is calculated and whose entropy is calculated as:

$$E = \frac{1}{q_j} \sum_{i=1}^{q_j} v_i \log v_i \quad \forall j = 1, \cdots, 20 \tag{1}$$

The parameter q_j is the number of measured coefficients in W falling on the *j-th* radial projection and v_i is the power of the *i-th* coefficient allowing to the *j-th* projection. Once calculated the entropy of each projection, the average value is chosen as a threshold value T. A *blade* composed by 9 parallel lines of k-space coefficients is collected around the projections whose entropy is above T (a sort of PROPELLER [17], [18]). Since the adaptive dataset follows the most informative directions, its shape is usually irregular. For this reason, the image is reconstructed by using a non linear reconstruction method. The dataset is suitable for non linear L_0-norm reconstruction [12], [15], in line with the theory of CS [13], [4]. Standard compressed sensing requires that, given an S-sparse image in some domain (in this case the Fourier domain), the number of measured k-space samples, Φf, must be $\Phi f > 2\mathrm{S}$ and, experimentally, $3\mathrm{S} \leq \Phi f \leq 5\mathrm{S}$ is usually chosen (having supposed that 5S is lower than M $\times$ M). On the other hand, the reconstruction method described in [11], [12] addresses directly the ideal L_0-norm minimization problem. This method minimizes iteratively continuous

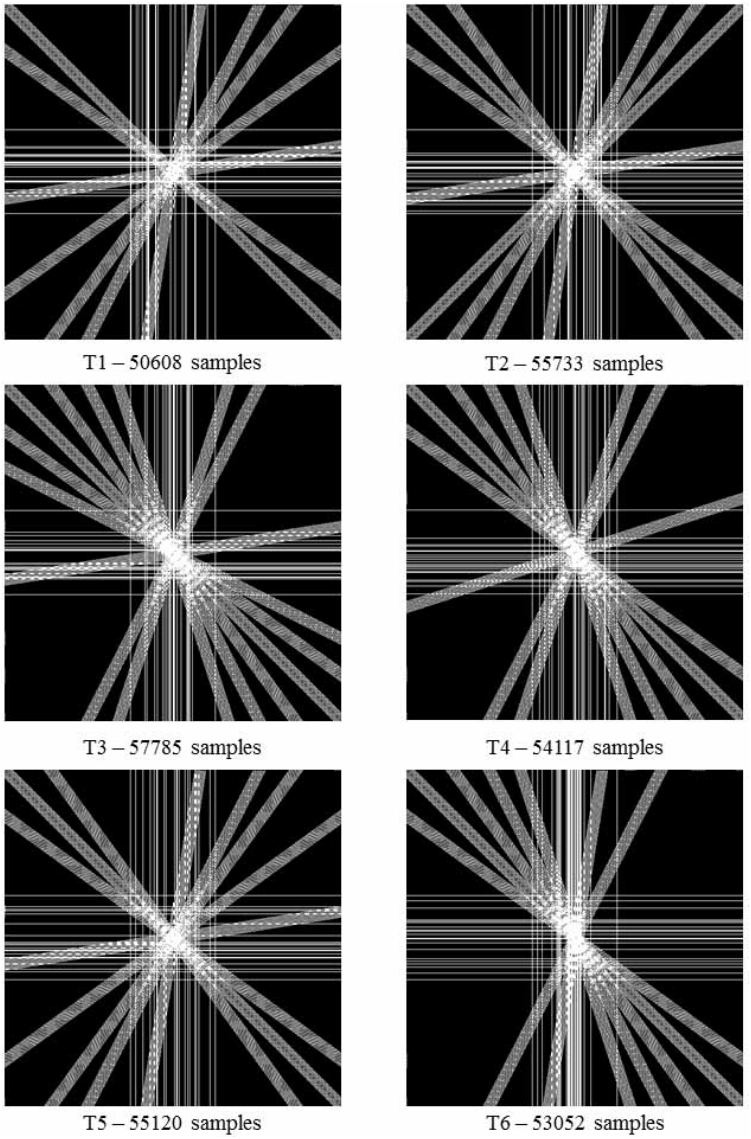

Fig. 4. Adaptive masks for T1:T6 obtained with $\sigma = 0.25$, p = M/4 and 20572 starting samples

approximations of the L_0-norm. Although the achieving of the global minimum is not ensured, the L_0-homotopic minimization method typically allows accurate image reconstruction by using a number of samples which is arbitrarily close to the theoretical minimum number for CS associated with direct L_0 minimization (2S measurements).

3 Numerical Experiments

Our aim is to demonstrate experimentally on cardiac MRI images that, by using the adaptive method and L_0-homotopic minimization, we can reconstruct an image with a number of samples very close to the sparsity coefficient, S, of the image without knowing a-priori the sparsity of the image (the value of S). In order to do that, we show how the weighted CS converges to the theoretical reconstruction, by using the L_0-homotopic minimization strategy, as the number of collected samples increases. Moreover, we show how important are, in the adaptive strategy, shape and cardinality of the starting dataset and how well the termination criterion allows to calculate the optimal number of coefficients. In order to do that, simulations have been performed on cardiac MRI completely sampled 512×512 images. To simulate the MRI acquisition, Fast Fourier Transform (FFT) of each image was performed and the obtained coefficients were treated as the k-space experimentally collected data, assuming that the image and the whole k-space dataset were not known a-priori (we found this procedure useful to compare the undersampled reconstructed images with the complete, theoretical, image). One of these images is reported on Figure 1(a). Figure 1(b) shows its Fourier coefficients (simulating k-space samples). Of the reported image, we also calculated the number of non-zero coefficients with respect to the total number: it was 51993 of a total of 262144 ($S = 51993$). The treated 25 images of the same subject, corresponding to 25 different phases of the cardiac cycle. Being the treated images very similar each other (the variations consisted in the movements of the heart), and very similar were also their S values ($S = 52750 \pm 2745$) and the acquisition/reconstruction results, we show and discuss just the results referred to the image reported in Figure 1.

For the reported image, at least 104000 samples would be necessary for CS to obtain a good reconstruction with L_0-homotopic minimization. To show this, we extracted a series of datasets, of different cardinality, for CS reconstruction. The datasets used for weighted CS were extracted by using a Gaussian weight extraction, both along the rows and the columns, in equal parts, in order to allow a more dense sampling in the central region of the k-space with respect to the peripheral zones. The Gaussian distribution function had zero mean and $\sigma = 1$. The number of samples in the extracted series of Gaussian weighted CS subsets gone from 30000 samples to 200000 samples (in step of 5000). These tests served to show how CS converged to the optimal reconstruction and to verify the correctness of the previously estimated sparsity value S, to allow a very good reconstruction, in a mean squared error (MSE) sense, with respect to the completely sampled image. The MSE values, calculated on the CS images reconstructed by using increasing datasets variations, are reported in Figure 2. Figure 2 (splitted in two to better visualize MSE variations) shows a strong non-monotonic behaviour between 30000 and 100000 samples, and a quite regular descendent behaviour above 105000 with reduced improvements above 150000. This demonstrates a sort of saturation, an arrival point, at about 150000 (about 3S). Moreover, at 115000, the MSE function showed a consistent decreasing: this number was very close to the optimal for CS (about 2S) for the given image. However CS, having no information about the image

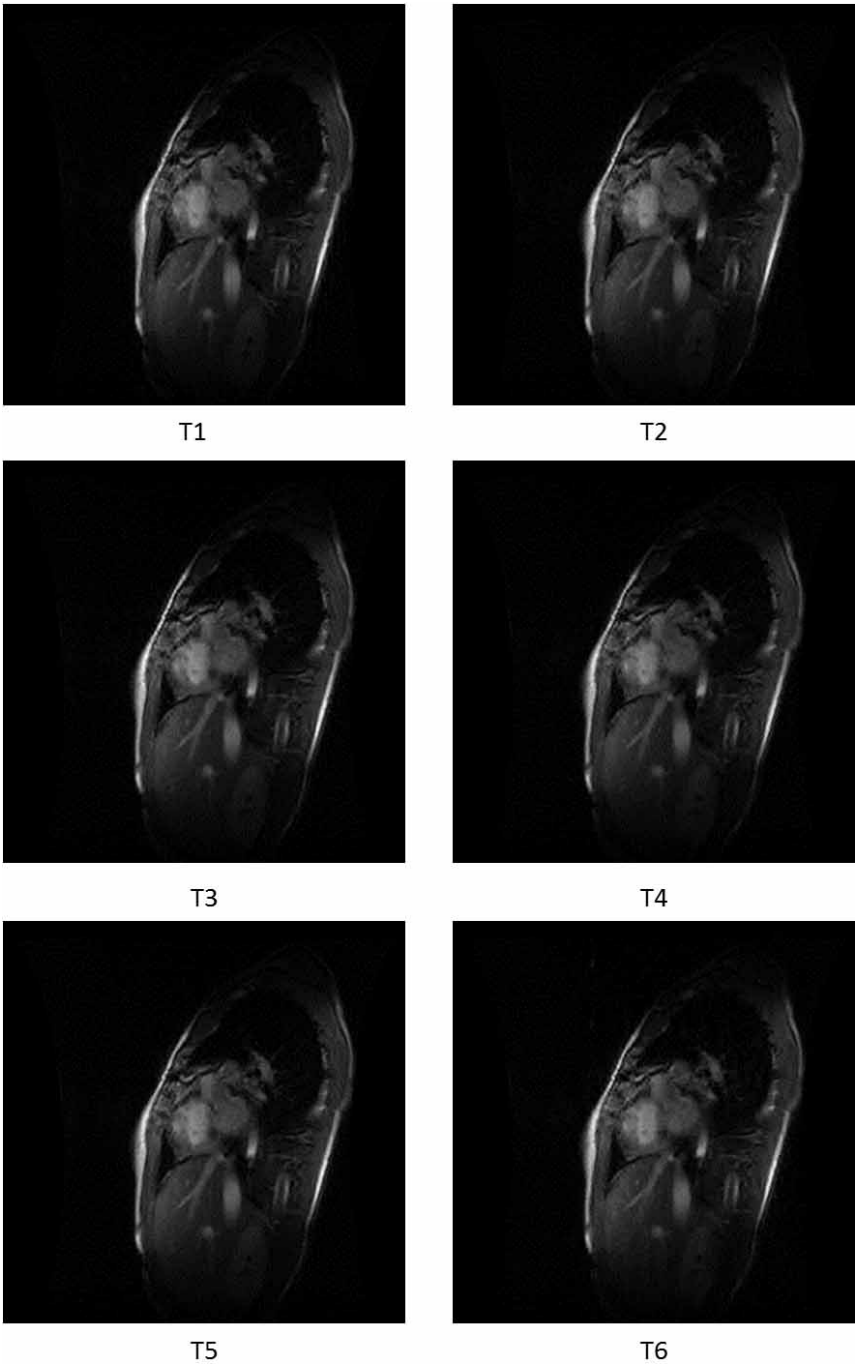

Fig. 5. Images reconstructed with the masks of Figure 4

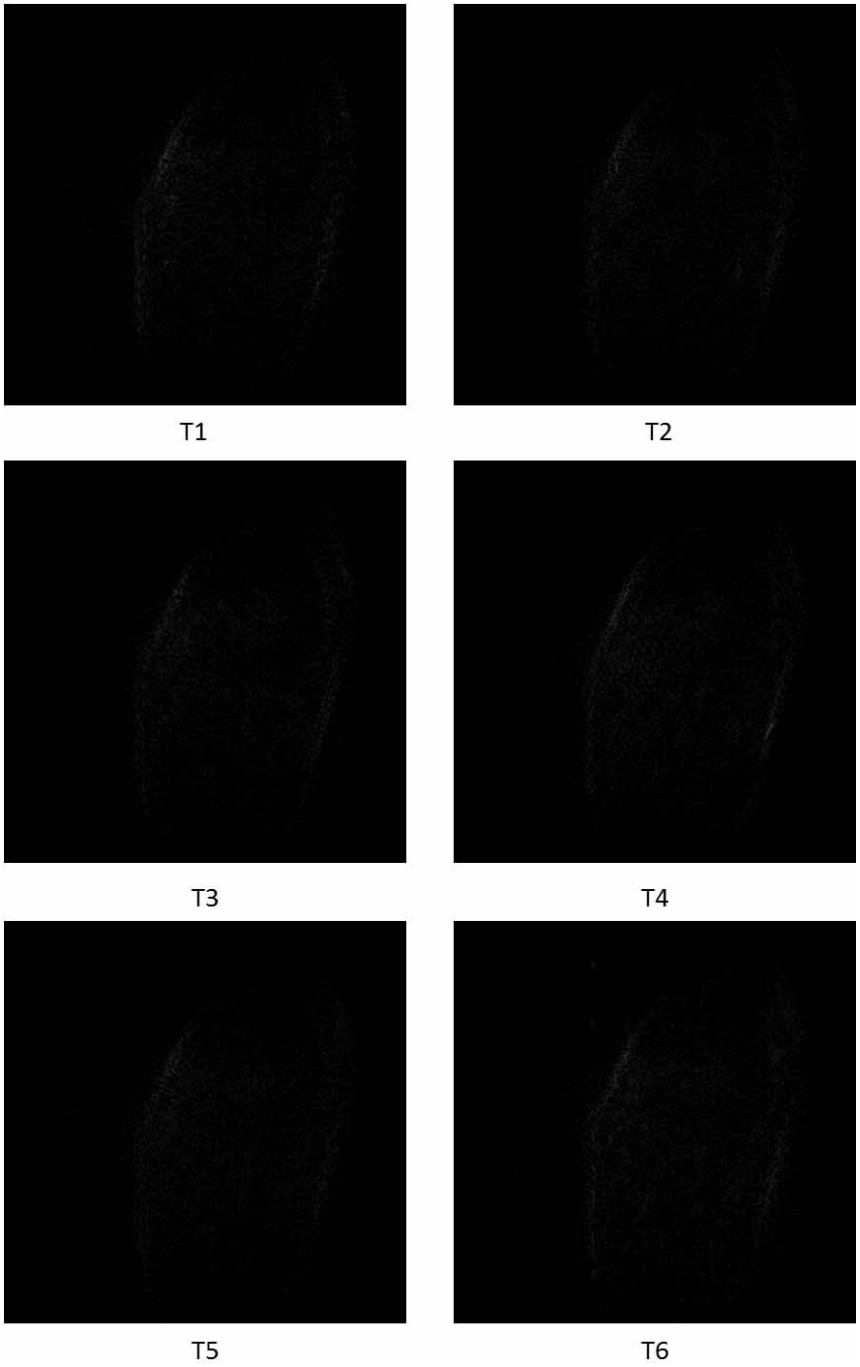

Fig. 6. Images obtained as difference between the theoretical image of Figure 1(a) and the images in Figure 5

shape and, hence, about this number, had no choice than to increase the number of collected coefficients above 2S. It is important to note that, for datasets between 50000 and 70000, besides noise, residual structured aliasing is present. The CS reconstruction with 115000 samples is reported in Figure 3(a). Figure 3(b) shows the difference between the theoretical image (Figure 1(a)) and the CS reconstruction (Figure 3(a)). Figure 3(b) confirms the good reconstruction without aliasing. Regarding the adaptive method, it requires that an initial, cross shaped, set of coefficients has to be used for entropy calculation to drive the acquisition of the following blades [15], [16], adaptively collected in base of their information content. The initial dataset has been proven to be crucial to include all the most informative directions of the image and two parameters are important: its extension (p) and the number of its coefficients. Having supposed that the center of the cross is located in the central region of the k-space, we performed different trials to verify that, starting from different datasets, the final adaptive datasets, were very similar. First, we choose a cross region where we extracted casually, with Gaussian distributions ($\sigma = 0.06$, $p = M/16$), rows and columns of k-space samples to generate 6 different datasets of about 10000 (10640) points. We used these datasets to perform 6 different adaptive acquisitions and reconstructions. From this first experiment, we noted that the final adaptive datasets were quite different both in shape and in the total number of the collected samples, thus demonstrating that the adaptive method, in most cases, was unable to collect the whole set of the most informative samples. This was mainly due to the fact that the starting datasets were too poor of samples and too narrow to capture all the dynamics of the whole image. For this reason, we repeated the experiments by increasing the starting number of coefficients to 20000 and by gradually increasing the width of the starting datasets ($\sigma = 0.06$ corresponding to $p = M/16$, $\sigma = 0.12$ and $p = M/8$, $\sigma = 0.25$ and $p = M/4$). For each setting of the parameters, 6 different starting mask were collected. Results are reported in Table 1. As can be noted (Table 1), in the last experiment ($p = M/4$, with 20572 starting points) the final number of samples in the adaptive datasets were similar and, more important, they were very close to the calculated value of S. Moreover, in this last example, whose final masks are reported in Figure 4, the obtained masks contained very similar directions, though using different casually collected Gaussian starting masks. This demonstrates that 20572 and $p = M/4$ can be considered acceptable parameters for the starting sets and that, with such starting sets, the adaptive method and its termination criterion allow to obtain a set of coefficients whose cardinality, 54400, is very close to 51993 (the sparsity value for this image). Figure 5 reports the images reconstructed with the masks of Figure 4. The image obtained as difference between the theoretical image of Figure 1(a) and those of Figure 5 are reported in Figure 6. Figure 7 reports the mask (Figure 7(a)) obtained as union of the 6 adaptive masks of Figure 4 and its reconstruction (Figure 7(b)). Figure 8 indicates the MSE values for the images of Figure 5 as compared to those calculated for the image reported in Figure 7 (obtained as union of the adaptive masks) and with that of Figure 3 (CS image reconstructed with 115000 samples).

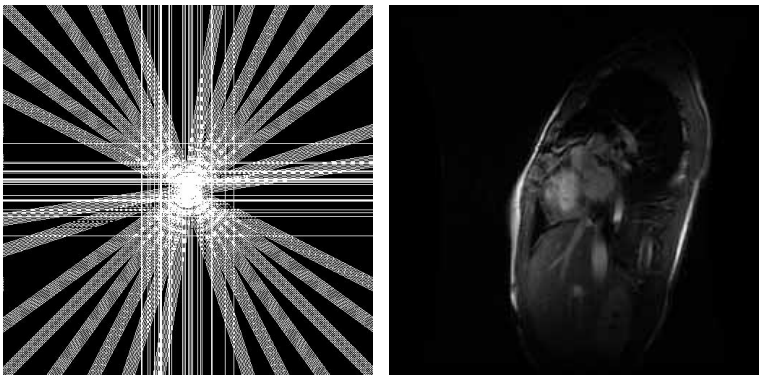

(a) (b)

Fig. 7. (a) Union mask (79066 samples) obtained as union of the masks T_1:T_6 of Figure 4, (b) image reconstructed by the using mask (a)

Table 1. Number of samples collected for the 6 trials (T_i) performed for each setting of the parameters

σ	p	Starting Points	T1	T2	T3	T4	T5	T6
0.06	M/16	20572	48092	54442	55082	55216	51282	54789
0.12	M/8	20572	54166	54149	56008	50968	58896	58340
0.25	M/4	20572	50608	55733	57785	54117	55120	53052

The adaptive method obtained good reconstructions (as confirmed by MSE values) without residual structured aliasing (as confirmed by analysing the reconstructed images), though it used very small datasets for reconstruction (their cardinality was very close to S). In particular, the obtained results were very similar to those obtained by the union of the adaptive masks or to the CS image obtained with 115000 samples. This demonstrates that the adaptive method allows to reduce the acquisition time of at least a factor of 2 with respect to the CS strategy. Moreover, the adaptive strategy demonstrates that also starting with different sets of samples, the method and the termination criterion allowed to converge to similar datasets, though with some difference. However, the differences included image similarities because all these final adaptive sets included the necessary information to recover good images (the union of the adaptive mask did not improve appreciably the reconstructed image).

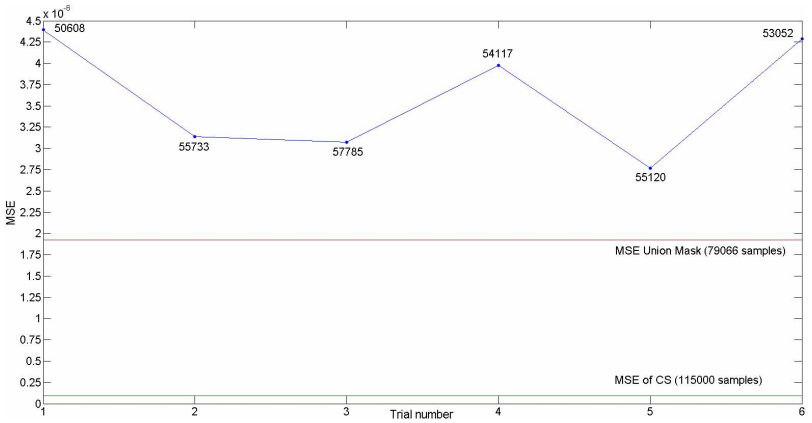

Fig. 8. MSE values for the 6 images of Figure 5, compared to the MSE error for the image in Figure 7 (obtained as the union of the adaptive masks, and composed by 79066 samples) and with the image in Figure 3 (CS image reconstructed with 115000 samples). MSE values for the union mask and CS were constant because each of them was referred to a single dataset.

4 Conclusions and Future Developments

An adaptive acquisition method for MRI has been applied to cardiac MRI images. The results of the proposed method were equivalent to weighted CS, through it used about half of the samples necessary for CS (CS results, for the same number of samples as the adaptive method, had worse MSE and produced residual structured aliasing). Through the performed experiments we demonstrated that with a starting mask obtained with $\sigma = 0.25$ and $p = M/4$ we obtained acceptable numbers and width for the starting sets. We also demonstrated that, with such starting sets the adaptive method and its termination criterion allowed to obtain a set of coefficients whose average number of coefficients was very close to the sparsity value and the reconstructed images were very similar to the original, completely sampled, image. Besides, it furnished a criterion to estimate the near optimal number of coefficients to obtain a good reconstruction for the given image: this was impossible for CS that, being it a blind method, required that the number of collected data had to be fixed in advance, independently of the image shape. For this reason, the adaptive method allowed to reduce the acquisition time of at least a factor of 2 with respect to the CS strategy: this is very important for cardiac imaging. In the future we plan to apply the proposed method on volumetric MRI datasets and to use spatial/temporal similarities and information to reduce further the number of collected samples.

References

1. O'sullivan, J.: A fast sinc function gridding algorithm for fourier inversion in computer tomography. IEEE Transactions on Medical Imaging 4(4), 200–207 (1985)
2. Placidi, G., Alecci, M., Sotgiu, A.: ω-space adaptive acquisition technique for magnetic resonance imaging from projections. Journal of Magnetic Resonance 143(1), 197–207 (2000)
3. Placidi, G., Alecci, M., Sotgiu, A.: Theory of adaptive acquisition method for image reconstruction from projections and application to epr imaging. Journal of Magnetic Resonance, Series A 108(1), 50–57 (1995)
4. Placidi, G.: MRI: essentials for innovative technologies. CRC Press (2012)
5. Placidi, G., Alecci, M., Colacicchi, S., Sotgiu, A.: Fourier reconstruction as a valid alternative to filtered back projection in iterative applications: implementation of fourier spectral spatial epr imaging. Journal of Magnetic Resonance 134(2), 280–286 (1998)
6. Candès, E.J., Romberg, J., Tao, T.: Robust uncertainty principles: Exact signal reconstruction from highly incomplete frequency information. IEEE Transactions on Information Theory 52(2), 489–509 (2006)
7. Donoho, D.L.: Compressed sensing. IEEE Transactions on Information Theory 52(4), 1289–1306 (2006)
8. Lustig, M., Donoho, D., Pauly, J.M.: Sparse mri: The application of compressed sensing for rapid mr imaging. Magnetic Resonance in Medicine 58(6), 1182–1195 (2007)
9. Elad, M.: Sparse and redundant representations: from theory to applications in signal and image processing. Springer (2010)
10. Usman, M., Prieto, C., Schaeffter, T., Batchelor, P.: k-t group sparse: A method for accelerating dynamic mri. Magnetic Resonance in Medicine 66(4), 1163–1176 (2011)
11. Trzasko, J.D., Manduca, A.: A fixed point method for homotopic l0-minimization with application to mr image recovery. In: Medical Imaging, International Society for Optics and Photonics, pp. 69130F–69130F (2008)
12. Trzasko, J., Manduca, A.: Highly undersampled magnetic resonance image reconstruction via homotopic-minimization. IEEE Transactions on Medical imaging 28(1), 106–121 (2009)
13. Lustig, M.: Sparse MRI. ProQuest (2008)
14. Wang, Z., Arce, G.R.: Variable density compressed image sampling. IEEE Transactions on Image Processing 19(1), 264–270 (2010)
15. Ciancarella, L., Avola, D., Placidi, G.: Adaptive sampling and reconstruction for sparse magnetic resonance imaging. In: Computational Modeling of Objects Presented in Images, pp. 115–130. Springer (2014)
16. Ciancarella, L., Avola, D., Marcucci, E., Placidi, G.: A hybrid sampling strategy for sparse magnetic resonance imaging. Computational Modelling of Objects Represented in Images III: Fundamentals, Methods and Applications, 285 (2012)
17. Pipe, J.G., et al.: Motion correction with propeller mri: application to head motion and free-breathing cardiac imaging. Magnetic Resonance in Medicine 42(5), 963–969 (1999)
18. Arfanakis, K., Tamhane, A.A., Pipe, J.G., Anastasio, M.A.: k-space undersampling in propeller imaging. Magnetic Resonance in Medicine 53(3), 675–683 (2005)